Modelling and Analysis of Voltage Distribution for Automated People Mover System in a Case Study of Suranaree University Technology Hospital Shuttle Service

J. Srivichai, T. Ratniyomchai, and T. Kulworawanichpong[*]

Abstract— *The power transmission to the automated people mover (APM) system under the limited voltage and the security conditions of the electric power supply system is seriously a sensitive problem of the power quality. Therefore, the performance analysis of the electric power supply system is important in the design and operation of the APM system, that the power load is usually dynamic. One of the main problems in the power supply station is the voltage drop due to the variation of the APM load according to the position of APM movement. This paper presents a modelling and analysis of the voltage distribution for the APM system. The model of the APM system for simulation is developed on the MATLAB/SIMULINK and the voltage regulation is evaluated by considering the percentage of voltage regulation between the traction substation and the APM vehicle. The results of this analysis, including the voltage regulation and energy loss for both 240 and 480 Vac systems, will be used as an evaluation guideline for the design and construction of the prototype APM system which is the shuttle services in the Suranaree University of Technology (SUT) Hospital as a case study.*

Keywords— **Automated people mover, traction power supply, voltage drop.**

1. INTRODUCTION

The APM systems are fully automated and driverless transit systems that operate on a fixed guideway in exclusive rights of way. APMs can include technologies called automated guideway transit (AGT). Typically, the APM uses wheel-on-rail/route systems and propulsion may involve conventional on-board electric motors, linear motors or cable traction. The system is controlled or monitored by operators from a remote central control facility. APM applications may partake names such as downtown people movers, airport APM, or automated trams depending on the operating environments [1].

The APM system consists of six components to support of the operated the passenger shuttle service system as follows [2]-[4]:

i. *The vehicle:* The APM system typically has a length of 10-12 m and a width of 3 m and capacity 50-80 passengers per train, which has a rubber wheel movement. It is a model that uses rubber wheels together with concrete running tracks, resulting in a cheap price and without noise, so it is often used in urban areas.

ii. *The guideway:* The guideway of the APM system is to supported running surface and controlling the direction of the APM vehicle to increase safety and efficiency in passenger transportation. The APM runway will consist of i) concrete runway for supporting the wheels of the vehicle, power distribution rail and direction rail or guide rail. There are two commonly used APM systems, classified by type of runway as follows:

i) central guide rail is a system that installs guide rail and power supply in the middle of the runway the width of the runway is about 3.2 m [5].

ii) side guide rail is a system to install guide rail and power supply rail on the runway the width of 1.85 m of wheels and when combined with the guide rail and electric rail installed on the side of the runway will have a width of 3.2 m [6].

iii. *The system power and propulsion:* The APM system receives electric power from the traction substations. Located along the path of the running track. The power distribution depends on the type of the APM driven. Self-propelled APM vehicle are electrically powered by onboard motors using either 750 or 1500 VDC or 480 or 600 VAC, distributed along the guideway by away side, rail-based power distribution subsystem. The primary electric system of the power supply system for the APM system generally depends on the selected system design on possibly both DC and AC systems [7]-[13].

iv. *The control systems:* All APM systems include command, control, and communications equipment needed to operate the driverless vehicles.

v. *The stations:* The stations are located along the APM 's running path. So that passengers can use the service comfortably. The station will be equipped with facilities such as automatic doors. Various information signs etc. for the convenience and safety of passengers. In addition, the station also has tools and equipment to support the APM system to work efficiently.

vi. *The maintenance and storage facility (MSF):* Items housed in the MSF include maintenance equipment, tool, machinery, recovery vehicle, equipment for train control and within the MSF, and any other equipment/systems

J. Srivichai is with the School of Electrical Engineering, Suranaree University of Technology, Nakhon Ratchasima 30000, Thailand.

T. Ratniyomchai is with the School of Electrical Engineering, Suranaree University of Technology, Nakhon Ratchasima 30000, Thailand.

T. Kulworawanichpong is with the School of Electrical Engineering, Suranaree University of Technology, Nakhon Ratchasima 30000, Thailand.

[*]Corresponding author: T. Kulworawanichpong; Phone: +66-88583-7207; E-mail: thanatchai@gmail.com.

associated with maintaining the APM vehicle.

Considering the research articles related to simulation for the APM system, the article [14] developed a sophisticated APM simulation model using the specialized simulation software EXTENDS. Their simulator, APMSIM, was capable of modeling passenger/vehicle movement, system performance, and energy consumption based on a number of input blocks. The simulation successfully allowed them to model energy consumption, waiting time, queues at stations, and many other variables of interest.

Regarding the prototype APM system in Thailand, the preliminary study and design of the characteristics of the electric drive system, shuttle route, and power supply system are to be carried out. Therefore, this paper studied and created the model of the vehicle movement, power supply through the conductor rail, and the power flow calculation of the APM system simulated in MATLAB/SIMULINK.

This paper is divided into six sections. Section one is an introduction. Section one is an introduction. Section two explains a basic calculation of the voltage regulation in an electric power system. Section three presents the traction performance calculation of the vehicle movement. Section four describes the model of the APM system, the programming sequence and algorithm for simulation using the proposed model. Simulation results addressing the test system and graphical illustration and conclusions are shown in section five and six, respectively.

2. VOLTAGE REGULATION

Regarding the electric power transmission system, the different voltage between the power supply and load terminals is the voltage drop on the power transmission line due to its parameters of resistance and inductance. This means that the receiving end voltage (V_r) of the line is generally less than the sending end voltage (V_s). The voltage drops ($V_s - V_r$) in the line is expressed as a percentage of the receiving end voltage V_r called the voltage regulation as follows [15]:

$$\% \text{ voltage regulation} = \frac{V_s - V_r}{V_r} \times 100 \qquad (1)$$

The voltage regulation can be defined as the proportional change in voltage magnitude at the load bus due to the load variation. The voltage drop is cased due to feeder impedance carrying the load current as illustrated in Fig. 1(a). If the supply voltage is represented by Thevenin's equivalent, then the voltage regulation (VR) is given by,

$$VR = \frac{\left| \bar{E} - \bar{V} \right|}{\left| \bar{V} \right|} \qquad (2)$$

where $\bar{V}$ is a phasor of the load voltage and $\bar{E}$ is a phasor of the power supply voltage. In Fig. 1(a), the source and load currents are equal and voltage drop due

to the feeder is given by,

$$\Delta \bar{V} = \bar{E} - \bar{V} = Z_s \bar{I}_l \qquad (3)$$

The feeder impedance, $Z_s = R_s + jX_s$. The relationship between the load apparent powers and its voltage and current is expressed below:

$$\bar{S}_l = \bar{V} I_l^* = P_l + jQ_l \qquad (4)$$

The load current is expressed as following

$$I_l = \frac{P_l - jQ_l}{V} \qquad (5)$$

Substituting I_l from equation 5 in equation 3

$$\Delta \bar{V} = \bar{E} - \bar{V} = \left(R_s + jX_s \right) \left(\frac{P_l - jQ_l}{V} \right) \qquad (6)$$

$$\Delta \bar{V} = \frac{R_s P_l + X_s Q_l}{V} + j \frac{X_s P_l - R_s Q_l}{V} \qquad (7)$$

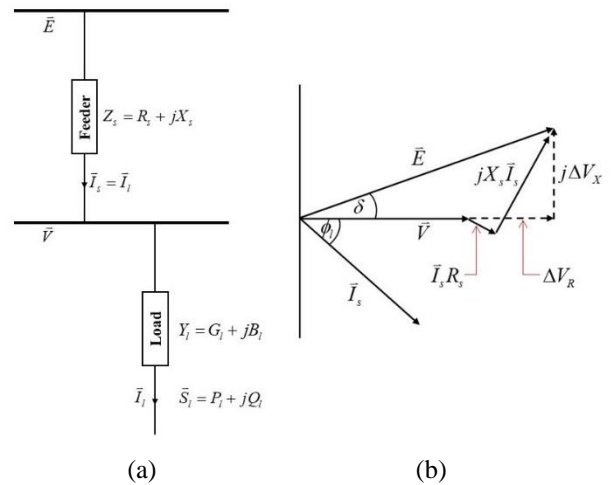$$\Delta \bar{V} = \Delta V_R + j\Delta V_X \qquad (8)$$

(a)   (b)

Fig. 1. (a) Single phase system with feeder impedance, (b) Phasor diagram.

Thus, the voltage drop across the feeder has two components, including phase ΔV_R and phase quadrature ΔV_X with the voltage V as illustrated in Fig. 1(a). The load bus voltage $\bar{V}$ depends on the feeder impedance, magnitude and phase angle of the load current. In other words, voltage change (ΔV_X) depends on the real and reactive power flows of the load and the feeder impedance. This situation is shown by the phasor diagram in Fig. 1(b).

3. TRACTION PERFORMANCE CALCULATION

Equations of movement

Vehicle movement is simply governed by the Newton's second law of motion as shown in equation 9 namely; the forces related are the tractive force, the gradient

force/gravitational force and the resistance forces. On the top of that, the resistance forces are subdivided into two forces consisting of the rolling resistance force and the aerodynamic drag force as in equation 10 [16]. Fig. 2 demonstrates the free body diagram of the vehicle moving upwards on the slope including the mentioned forces exerting on it

$$F_{TE} - F_R - F_G = M_{eff} a \qquad (9)$$

$$F_R = F_{rr} + F_{drag} \qquad (10)$$

where F_{TE} denotes the tractive effort (*N*), F_R denotes the resistance force (*N*), F_G denotes the gradient force (*N*), F_{rr} denotes the rolling resistance force (*N*), F_{drag} denotes the aerodynamic drag force (*N*), a denotes the vehicle acceleration (*m/s²*), M_{eff} denotes the effective mass which is equal to $M_t(1 + \lambda_w) + M_l$ where M_t denotes the tare mass (*kg*), λ_w denotes the rotary allowance, M_l denotes the passenger load (*N*), and a denotes the acceleration rate (*m/s²*).
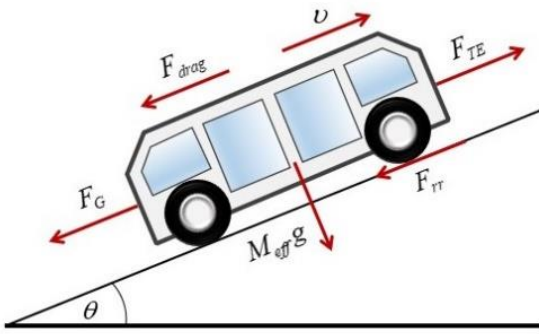

Fig. 2. Free body diagram of the vehicle movement.

In addition to rolling frictional resistance and aerodynamic drag force, the basic resistance of the vehicle is also affected by the friction of the bearing, the relative sliding of the rubber wheel and the cement pavement, the impact and vibration of the rubber wheel and the road surface. Therefore, the Davis's equation is often used in engineering to estimate the resistance force [14].

$$T_{rd} = \frac{F_{rr} + F_{drag}}{M_{eff} g}$$

$$= 5 \times 10^{-4} K_0 + 4.4480 \frac{K_1}{w \times 10^{-3}}$$

$$+ 1.1187 \times 10^{-3} B(\upsilon) + 239.6904 \frac{CA(\upsilon^2)}{wn \times 10^{-3}} \qquad (11)$$

where T_{rd} is the total resistance force (*N/N*), w is vehicle axle weight (*kg*), A is the projected frontal area of the vehicle (*m²*), B is empirical coefficient related to guideway conditions, C is drag coefficient, n is number of axle, and υ is the speed of the air relative to the vehicle body (*m/s*).

K_0 and K_1 are constant coefficients, which are adopted by 1.3 and 29, respectively.

Gravity is another factor that has been considered separately. As a result of the mass of the vehicle moving on the runway that is inclined at an angle to the running surface. There may be directions to support the movement or to resist movement. The mathematical representation of the gradient force is expressed as follows:

$$F_G = M_{eff} g \sin \theta \qquad (12)$$

where g is gravitational constant (9.81 *m/s²*), and θ is the angle of the slope (in degree).

Power consumed by a vehicle

The power consumed by a vehicle corresponding to tractive effort F_{TE}, instantaneous speed υ, and auxiliary power P_{aux} (such as air-conditioning load and on-board power service, etc.) is given by the following expression [16].

$$P_e = \frac{F_{TE} \times \upsilon}{\eta_t} + P_{aux} \qquad (13)$$

Where, η_t is the efficiency of conversion of electrical input power to the mechanical output at the wheels.

Speed and position up date

Once the vehicle acceleration is obtained, speed and position of the vehicle is calculated by the following equations,

$$\upsilon(t + \Delta t) = \upsilon(t) + a\Delta t \qquad (14)$$

$$s(t + \Delta t) = s(t) + \upsilon(t)\Delta t + \frac{1}{2} a\Delta t^2 \qquad (15)$$

where $\upsilon(t + \Delta t)$ and $\upsilon(t)$ are the terminal and initial speed, Δt is the time step which is 0.1 sec in this paper, $s(t + \Delta t)$ and $s(t)$ are the position after and before updated.

Summary of vehicle movement calculation

According to the flowchart in Fig. 3, the vehicle movement calculation can be summarized as follows: i) determine the gradient force, vehicle resistance, etc. and then compute the vehicle acceleration in equation 9-12, ii) use the speed from the previous time update to evaluate the tractive effort and thus the power consumption in equation 13, and iii) update the APM speed and position in equation 14-15.
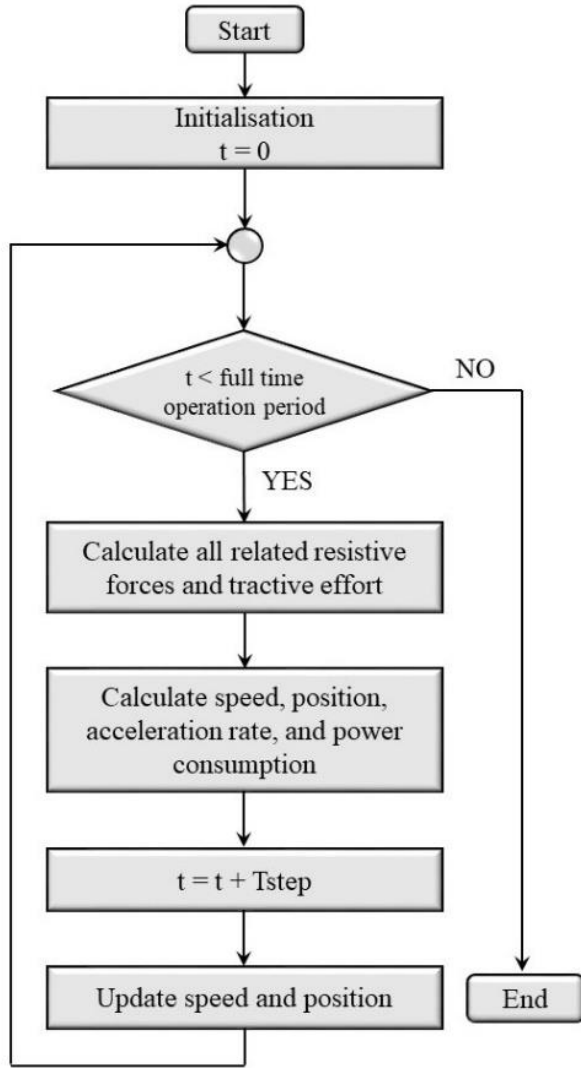
Fig. 3. **The flowchart of the vehicle movement calculation.**
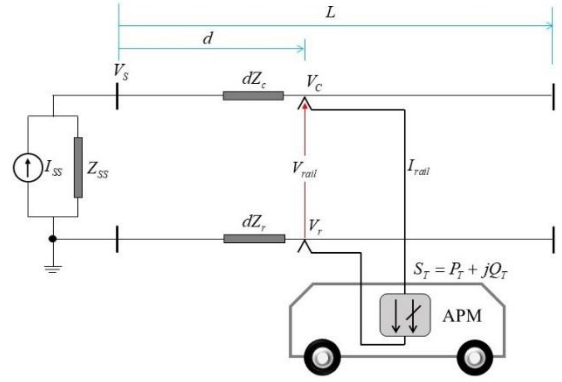

Fig. 4. Equivalent circuit of an AC power supply system.

In normal traction mode, the equivalent circuit of the APM is show in Fig. 4. The substation energy consumption is computed by integrating all substation instantaneous power over the APM operation time, as shown in equation 17.

$$E_{sub} = \int_0^T V_s I_{ss} \, dt \qquad (17)$$

where E_{sub} is the substation energy consumption (kWh), T is the total time of the APM operation (sec), V_s is the voltage of a substation (V), and I_{ss} is the current of a substation (A).

APM receive the electricity from current collector which connect with the conductor rail. The train power depends on the voltage and current at the current collector, which is solved by a load flow solver. Thus, the train energy can be computed by integrating APM instantaneous power over the time, as shown in equation 18.

$$E_{APM} = \int_0^T V_{rail} I_{rail} \, dt \qquad (18)$$

where E_{APM} is the APM energy consumption at the current collector (kWh), T is the total time of APM operation (sec) including both travelling time and dwelling time, V_{rail} is the voltage of the transmission conductor (V), and I_{rail} is the current of the transmission conductor (A). Energy consumption of train is usually primarily measured or calculated at the pantograph level, the intake to the train. However, the energy needed at the train's pantograph causes energy losses in the power supply system. In order to estimate the energy being consumed in the APM system as a result of a specific APM operation, these losses should be added to the energy intake to the APM. The loss of the power supply system is dependent on the power load, which varies over time. In this study, however, we will estimate and consider the average losses in the system. If the utilized energy is E_{APM} at the current collector and the energy intake is E_{sub} the energy loss is represented as follows [17]:

$$E_{loss} = E_{sub} - E_{APM} \qquad (19)$$

4. MODELING AND SIMULATION PROCEDURE

In this topic, presents the AC power supply system for APM. The equivalent circuit of AC power supply systems is summarized shown in Fig. 4, the substation is modeled by Norton's equivalent source [16] in which I_{ss} and Z_{ss} represent the Norton's short-circuit current and Norton's resistances, respectively; the voltage drop calculation is represented as follows:

$$V_{rail} = V_c - V_r = I_{ss} Z_{ss} - \left[Z_{ss} + d \left(Z_c + Z_r \right) \right] I_{rail} \quad (16)$$

where Z_c and Z_r are the per-unit impedance of the conductor rail (Ω/m) for the supply rail and current-return rail, respectively, d is the distance of the vehicle from the substation (m), L is the length of the conductor rail (m), and I_{rail} is the current which return to the substation through the conductor rail (A).

The relative loss e_{loss} is determined by

$$e_{loss} = \frac{E_{loss}}{E_{sub}} \qquad (20)$$

The energy efficiency η_{loss} is then determined by

$$\eta_{loss} = \frac{E_{APM}}{E_{sub}} \qquad (21)$$

or $\qquad \eta_{loss} = 1 - e_{loss} \qquad (22)$

Also, e_{loss} may be determined by

$$e_{loss} = 1 - \eta_{loss} \qquad (23)$$

APM traction power supply modelling in MATLAB/ SIMULINK

The model of the traction transformer, conductor rail, and APM are modelled by using the built-in blocks in MATLAB/SIMULINK. The configuration of The APM power supply system is briefly mentioned. Lastly, the evaluation of the voltage regulation at the traction substation and APM with different scenarios of the APM operations is discussed as follows:
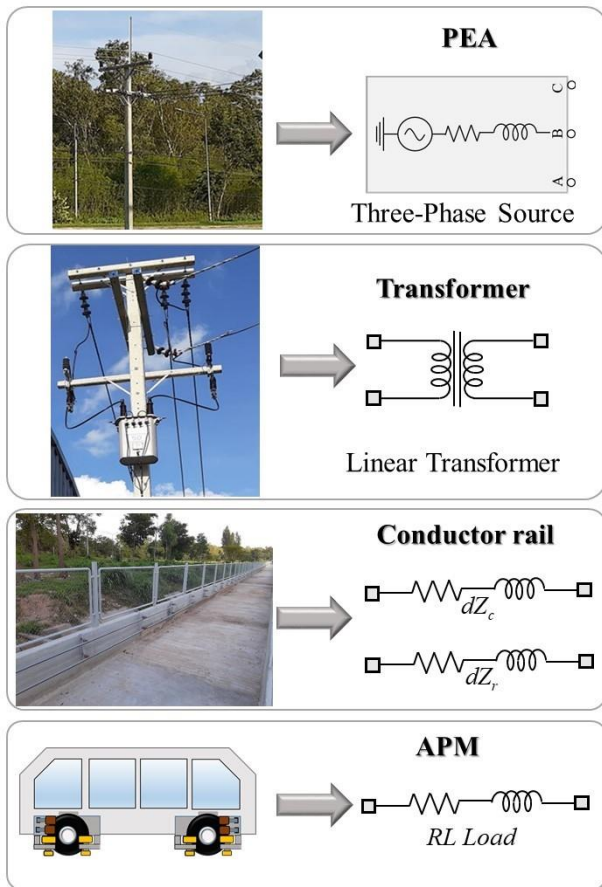
Fig. 5. The power feeding components models in MATLAB/SIMULINK.

The AC traction power supply modelling is developed in the block models in MATLAB/SIMULINK. The model consists of 4 main parts: i) AC traction substation,

ii) transformer, iii) conductor rail system, and iv) APM as shown in Fig. 5, The 22 kV AC transmission system as the traction substation is represented by the three-phase source built-in block. The transformer will step down the voltage from 22 kV to 240 V using the linear transformer built-in block. The conductor rail has the impedances obtained from the datasheet [18] modelling by the series RLC branch built-in block. Lastly, the APM is modelled as a series RLC load.

The APM system is modelled for the simulation in this paper. The APM was the first vehicle operated with conductor rail contact system to commence operations in Thailand. The APM is composed of two passenger stations and one traction substation as shown in Fig. 6. Parameters setting for this simulation can be found in the Appendix.

Fig. 6. SUT Hospital shuttle service [19].

The AC traction substation of the APM draws the electrical energy with the voltage level of 22 kV from the provincial electricity authority (PEA). The traction substation transformer with an alternate phase connection steps down the grid voltage into the APM's nominal voltage of 240 V. The total shuttle service distance is 200 m.

Simulator Structure

The operating diagram is shown in Fig. 7. The simulator has two major parts: the main program (script M-file) and the power network solver (SIMULINK). The main program performs the APM train movement and performance calculation. Then, the APM's positions and powers together with the distances recently mentioned are transferred into the SIMULINK block model to solve the voltage solution, consumed power and power losses etc. Finally, those values are returned to the main program to be stored and display the graphical illustration.
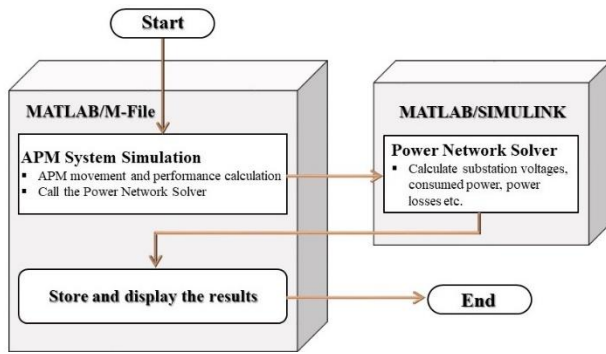
Fig. 7. Diagram of the simulation program.

5. SIMULATION RESULTS AND DISCUSSION

The simulation of the APM system is intended to observe the variation in voltage between measured point of the substation and the APM. as shown in Fig. 8. The results of the study are shown as follows:
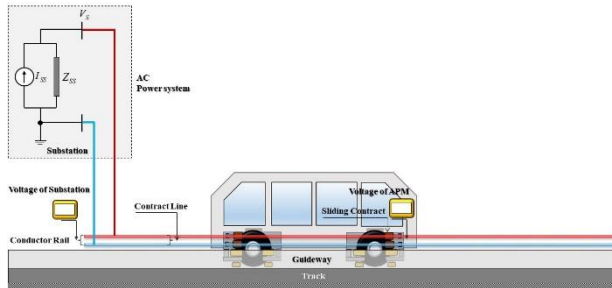

Fig. 8. **The position of the voltage measurement point.**

The APM speed control is governed by the proportional control that calculates the acceleration rate by the speed mismatch between the speed at the present time and command speed per time step, 0.1s in this paper. Only accelerating, constant speed, and braking modes of motion are considered. The gradient profile data is given and gradient force is also taken into account. The permissible maximum of the simulation time or the final time is 80.5 seconds for the round-trip. The expected results obtain the APM's speed profile, power and voltages at the substation, the voltage profile of the APM, power losses, and cumulative energy of the APM system shown in Fig. 9-16.
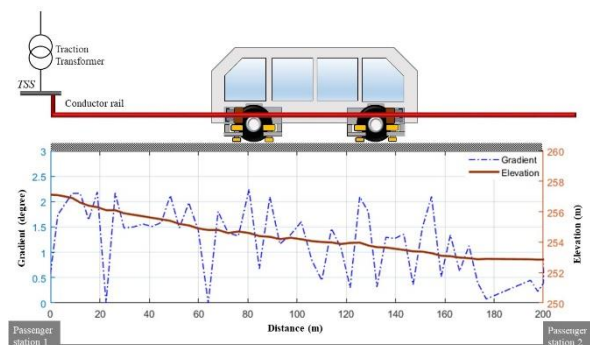
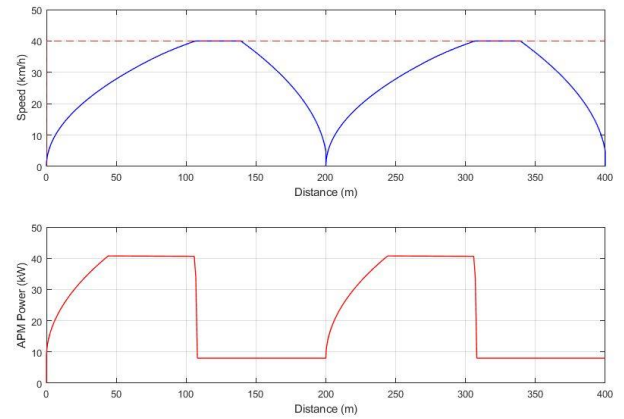**Fig. 9**. **Route vertical alignment and station.**

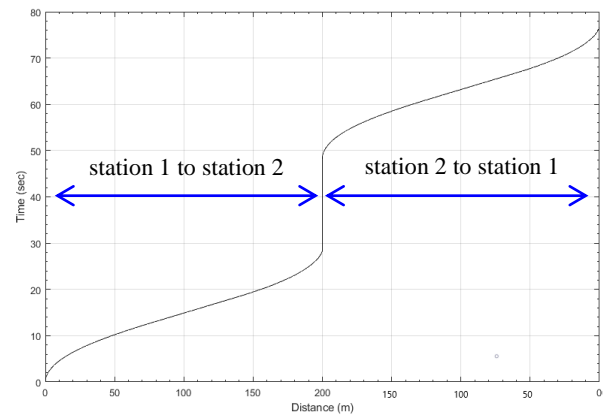**Fig. 10**. **The speed profile and power of the APM.**

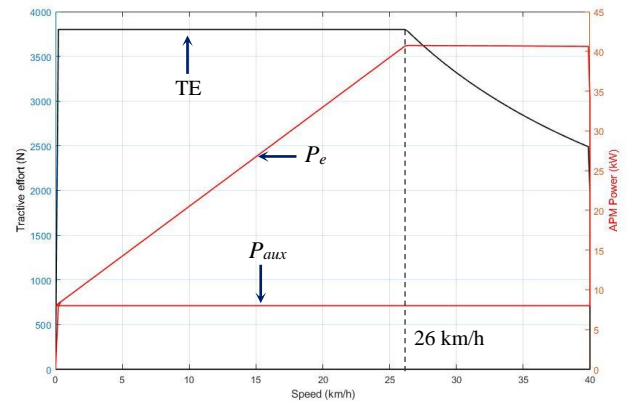**Fig. 11. Distance-time curve of APM service.**

Fig. 12. Tractive force and speed curve of the APM.

A diagram of the route vertical alignment and passenger station is shown in Fig. 9; the gradient profile in the figure was obtained from a GPS tracking device. In Fig. 10 present the APM speed along the distance it moves following with the red dot-line served as the arbitrarily specified speed command. The APM draws power during acceleration and speed control mode for tractive purpose and consumes only the auxiliary power during stopping at the station as shown in Fig. 10. Fig. 11 shows the distance-time curves from these simulation for the round-trip of the APM system simulator. The tractive effort curve in Fig. 12 describes the relationship between tractive effort and speed curve.
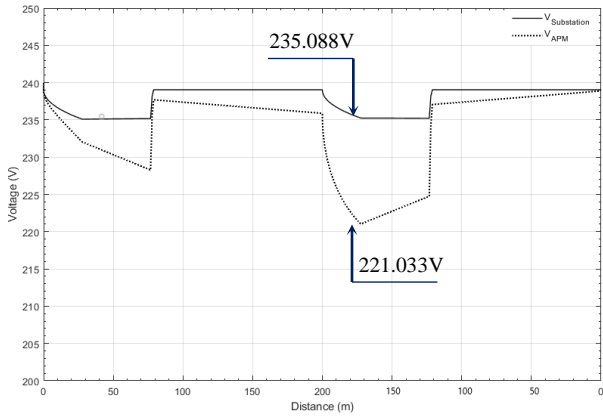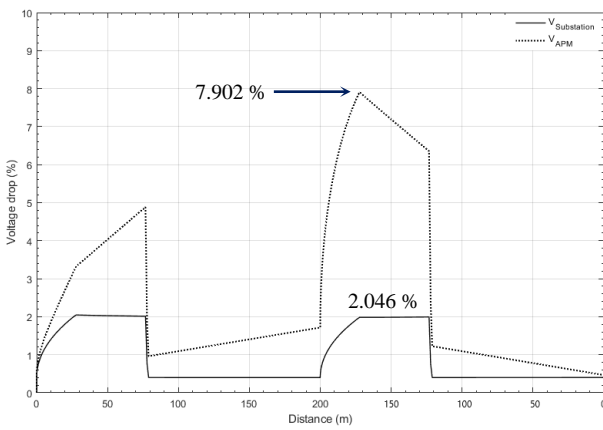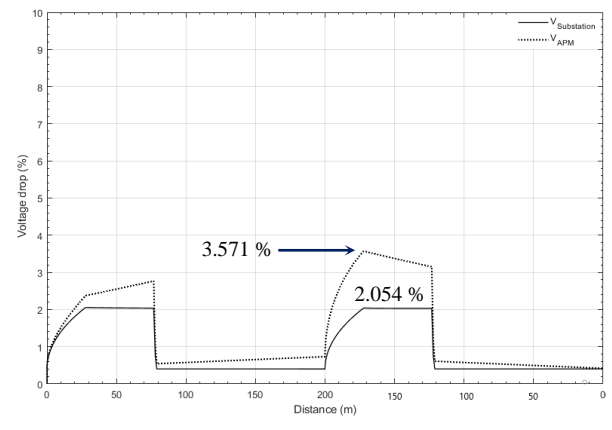
(a) 240 VAC
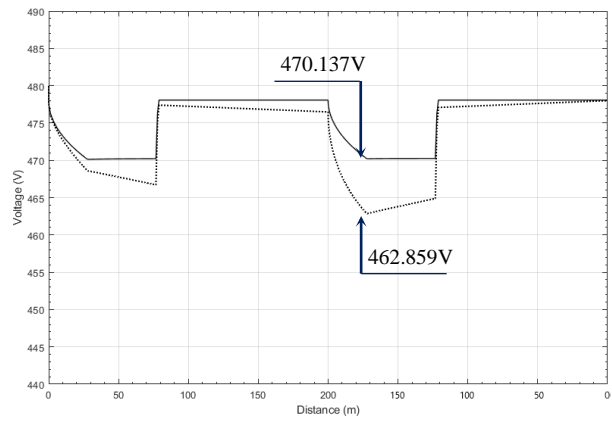
(b) 480 VAC

Fig. 13. The voltage regulation between the substation and APM with the power feeding system.
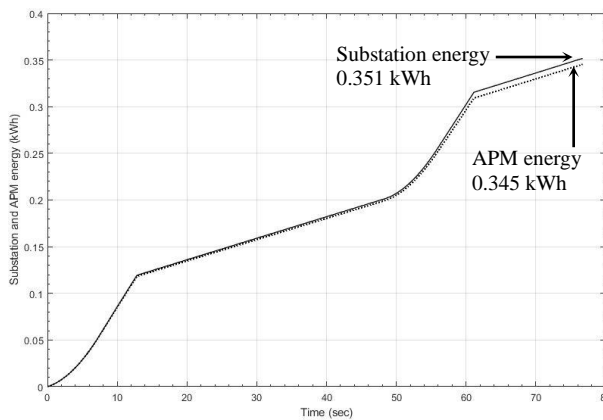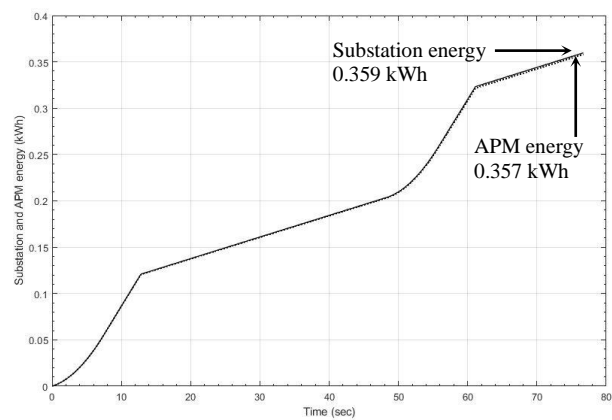

(a) 240 VAC

(b) 480 VAC

Fig. 14. Percentage of voltage regulation with the power feeding system.

(a) 240 VAC

(b) 480 VAC

Fig.15. The cumulative energy of APM system.
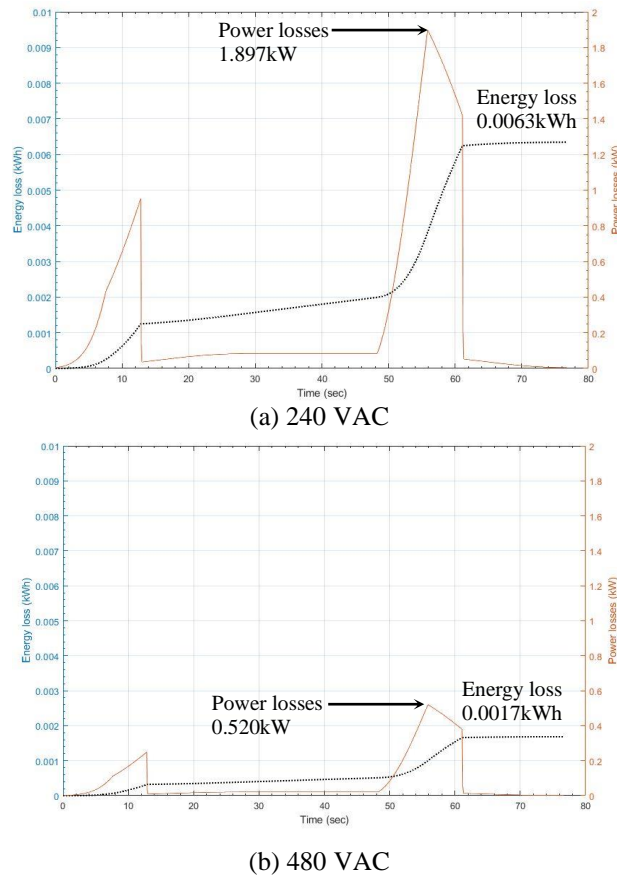
(a) 240 VAC

(b) 480 VAC

Fig. 16. Losses in the APM system for power feeding systems.

Voltage characteristics are shown in Fig. 13-14, while the APM moves to the terminal station at a distance of 200 m and then returns back to the first station, it is found that the minimum voltage at the traction substation and the APM in 240 VAC system are 235.088 V and 221.033 V respectively and 480VAC system is 470.137 V and 462.859 V respectively see in Fig. 13(a)-(b). Regarding the evaluation as a percentage according to the first equation above, it found that the maximum percentage of the voltage drop at the traction substation and the APM with 240V AC power feeding system is 2.046% and 7.902% respectively and 480 VAC system is 2.054% and 3.571% respectively see in Fig. 14(a)-(b). The main causes of the voltage drop in this case study are rail impedance, vehicle tractive load, and instantaneous vehicle distance. As seen in Fig. 13 and 14, the voltage drop increased with both the vehicle distance and tractive load. It is obvious that the voltage drops during acceleration in the return trip resulted in a huge voltage drop. Unlike the voltage drop at the vehicle, the substation voltage was not influenced by rail impedance, hence much less voltage drop. As a result of 480 VAC power feeding system, the percentage of the voltage drop does not exceed the standard [20]. The accumulative energy and energy loss of the APM system are shown in Fig. 15 and 16. The total energy consumption greatly rose on the return trip because the vehicle demanded high electrical power and energy from the substation as well as high losses in the supply rails

during acceleration from the other end of the supply feeder.

The total simulation results for these tests are summarized in Table 1. The energy loss percentage is 0.473 for 480 VAC, whereas, it is 1.790 for 240 VAC system.

Table 1. Summary of the simulation runs

Specification	Power Feeding System	
	240VAC	**480VAC**
voltage at the substation (V)	235.088	470.137
voltage at the APM (V)	221.033	462.859
voltage at the substation (%)	2.046	2.054
voltage at the APM (%)	7.902	3.571
substation energy (kWh)	0.351	0.359
APM energy (kWh)	0.345	0.357
power losses (kW)	1.897	0.520
energy loss (kWh)	0.0063	0.0017
relative loss (kWh)	0.0179	0.0047
energy loss (%)	1.790	0.473

6. CONCLUSION

During the planning and design for the APM system, it is essential to study the traction power system. According to the simulation results, the 480 VAC system has many advantages over the 240 VAC system. The advantages considered are the voltage drop characteristics and the low energy loss of the 480 VAC system. The simulation showed that the voltage drop percentage and traction energy loss percentage of the 480 VAC system is half those of the 240 VAC system. Therefore, the simulation and analysis results can be a guideline in the selection and design of a voltage distribution system for the APM system. In the future, the simulation in this study can be used to find the optimal position of an APM traction substation with the minimized power loss and voltage drop.

REFERENCES

[1] Wikipedia. Automated Guideway Transit. [On-line serial], Retrieved October 9, 2018 from the World Wide Web: https://en.wikipedia.org/wiki/Automated _guideway_transit

[2] ACREP Report. 2010. Guidebook for Planning and Implementing Automated People Mover Systems at Airports. Transportation Research Board. Washington, D.C.

[3] Akimura S. 2013. Japan's urban transport policy & The new transport system (NTS). Japan Transportation Planning Association.

[4] Liu, R. 2017. Automated Transit: Planning, Operation, and Applications. John Wiley & Sons, Inc, Hoboken, N.J.

[5] Bombardier. People mover. [On-line serial], Retrieved June 9, 2019 from the World Wide Web: https://rail.bombardier.com/en/solutions-and-technologies/urban/people-mover.html.

[6] Mitsubishi Hevy Industries Engineering. Transportation. [On-line serial], Retrieved June 9, 2019 from the World Wide Web: https://www.mhiengineering.com/products/transport.html.

[7] Horn, K. and Richardson, R. 2010. Guidebook for Planning and Implementing Automated People Mover Systems at Airports. Airport Cooperative Research Program.

[8] Kobe Steel, Ltd. Automated Guideway Transit System. [On-line serial], Retrieved August 2, 2019 from the World Wide Web: http://www. http://staff.washington.edu/jbs/itrans/Yuki%20Matsuoka-AutomatedGuidedTransit.pdf

[9] Hiroyuki, M. et al. 2003. Automated People Mover System Crystal Mover for Singapore's LTA. Mitsubishi Heavy Industries, Ltd. Technical Review Vol. 40, No. 3, pp. 1-10.

[10] SEKIYA, T. and ODA, Yo. 2007. First Transportation Project APM System for Hong Kong International Airport. IHI Engineering review. Vol. 40, No. 1.

[11] Paul, Lo. 2005. APM System AC Traction Power Supply System. Senior Electrical Engineer MTR Corporation.

[12] Final Report. 2018. Study on Transport System Among Terminals in Delhi Airport in India. Ministry of Economy, Trade and Industry, Nippon Koei Co., Ltd.

[13] Raney, S., & Young S. 2004. Morgantown People Mover-Updated Description. Advanced Technology Research Engineer Kansas Department of Transportation.

[14] Lin, Y.-D., & Trani, A. A. 2000. Airport Automated Poeple Mover Systems Analysis with a Hybrid Computer Simulation Model. Transportation Research Record (1703), pp. 45-57

[15] Kassu, B. 2017. Assessment and Mitigation of Voltage Drops on Traction Lines: Case Study of Sebeta-Adama Line. Ph.D.Thesis, Addis Ababa University, Addis Ababa Ethiopia.

[16] Kulworawanichpong, T. 2017. Railway Electrification. SUT 1st Edition. Suranaree Universtty of Technology.

[17] Andersson, E. and Lukaszewicz, P. 2006. Energy consumption and related air pollution for Scandinavian electric passenger trains. Department of Aeronautical and Vehicle Engineering Royal Institute of Technology, KTH.

[18] MARCH, MHS Rigid Conductor Bar Series. [On-line serial], Retrieved August 9, 2019 from the World Wide Web: http://www.march-china.com.

[19] Master Plan for Building Group. Suranaree Universtty of Technology Hospital.

[20] Conductors-Minimum Ampacity and Size. 2014. NEC Standard 210.19(A).

[21] Fact Sheet Transformer. Precise Electric Manufacturing Co., Ltd.